Journal of Materials Chemistry A

Accepted Manuscript

This article can be cited before page numbers have been issued, to do this please use: J. Piella, F. Merkoçi, A. Genc, J. Arbiol, N. G. Bastús and V. puntes, *J. Mater. Chem. A*, 2017, DOI: 10.1039/C7TA01328K.

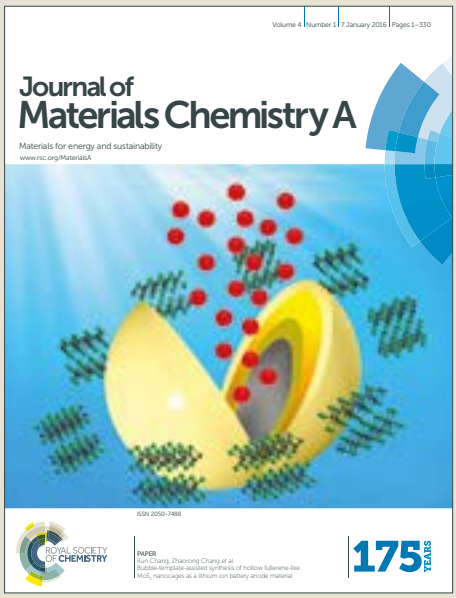

ROYAL SOCIETY OF CHEMISTRY

rsc.li/materials-a

View Article Online
DOI: 10.1039/C7TA01328K

Probing the Surface Reactivity of Nanocrystals by the Catalytic Degradation of Organic Dyes: The Effect of Size, Surface Chemistry and Composition.

Jordi Piella[a,b], Florind Merkoçi[a], Aziz Genç[a], Jordi Arbiol[a,c], Neus G. Bastús[a*] and Victor Puntes[a,c,d]

[a] Institut Català de Nanociència i Nanotecnologia (ICN2), CSIC and The Barcelona Institute of Science and Technology (BIST), Campus UAB, 08193, Bellaterra, Barcelona, Spain.
[b] Universitat Autònoma de Barcelona (UAB), Campus UAB, 08183 Bellaterra, Barcelona, Spain
[c] ICREA, Pg. Lluís Companys 23, 08010 Barcelona, Catalonia, Spain
[d] Vall d'Hebron Institut de Recerca (VHIR), 08035, Barcelona,

* To whom correspondence should be addressed: E-mail: neus.bastus@icn2.cat

ABSTRACT

We herein present a comprehensive study on how the catalytic performance and reusability of Au nanocrystals (NCs) are affected by systematic variations of crystal size, surface coating and composition. The reduction of different organic dyes (4-Nitrophenol, Rhodamine B and Methylene blue) by borohydride ions were used as model catalytic reactions. The catalytic performance of the Au NCs ranged between 3.6 to 110 nm was found to be dependent on crystal size, indicating that Au surface atoms have a distinct size-dependent reactivity in this reaction. Similarly, catalytic performance was found to be strongly dependent on the nature of the coating molecule, obtaining lower catalytic activities for molecules strongly bounded to Au surface. Finally, catalytic performance was found to be dependent on the chemical composition of the NC (Au, Ag, Pt) and the model dye used as a testing system, with the highest degradation rate found for Methylene blue, followed by 4-Nitrophenol and Rhodamine B. We believe that this study provides a better understanding of the catalytic performance of Au NCs upon controlled modifications of structural and morphological parameters, and working environment that can be used to facilitate the selection of the optimum NC size, coating molecules and evaluation systems for a particular study of interest.

View Article Online
DOI: 10.1039/C7TA01328K

INTRODUCTION

Recent advances in the ability to design and develop synthetic strategies for the production of colloidal metal nanocrystals (NCs) with controlled morphologies and well-defined facets and structures allows for tuning of their physicochemical properties and for optimizing their activity. This unprecedented morphological control is extremely useful in a variety of applications[1-3] , particularly in the case of heterogeneous catalysis, which can benefit from significant enhancements in catalytic activity and/or selectivity along with a significant reduction in the amount of employed material.[4-6] However, most of the catalysts used in industrial applications are still composed of polycrystalline NCs with poorly defined facets and broad size and shape distributions. These NCs of different morphological characteristics present distinct reactivity, attributable to the exposition of different crystallographic facets and fraction of surface atoms, which ultimately affects their performance independently of the catalytic reaction of study.[7]

In general, the reduction of particle size leads to an increase of catalytic performance due to the larger surface-to-volume ratio of smaller NCs.[8, 9] In addition to the fraction of atoms exposed, the performance (activity[10] and selectivity[9, 11]) of the catalyst is also determined by the availability and coordination of these atoms. Thus, low coordinated atoms in small NCs may exhibit much higher catalytic activity than highly coordinated ones due to a greater density of unsaturated atomic steps, ledges, and kinks which can serve as active sites for breaking chemical bonds.[12, 13] However, very active surface atoms can also result in NCs being unstable during the course of their catalytic function. NCs have a strong tendency to minimize their total surface energy and thus, structures with higher surface energies are more prone to surface reconstruction, sintering and aggregation which may ultimately compromise the long-term catalytic performance and reusability of the catalyst.[7]

Size-dependent catalysis by colloidal metal NCs have been widely studied for different systems, including CO and alcohol oxidation[14-16], selective hydrogenation[17] and reduction of hexacyanoferrate (III) ions[18], 4-Nitrophenol[19] and eosin[20]. However, direct relationships between size and catalytic function are missing or have been difficult to extract since the NCs studied, particularly in the small size regime, were heterogeneous (lack of control of NC size and comparison of NCs with different surface chemistry) and/or because the use of model systems dissimilar to working catalysts. Besides, the presence of the by-products in the reaction mixture, and the synthetic chemical environment in which they were produced (pH, concentration and surfactant) affected the final catalytic activity of NCs.[21] Therefore, an important requirement for comparing size-dependent catalytic effects is the precise control of NC size and morphology following highly reproducible and robust techniques.

View Article Online
DOI: 10.1039/C7TA01328K

Additionally, an issue that has not been sufficiently addressed is the role of the outer organic shell, i.e., the presence of capping agents normally used to control NC growth and stabilize the NCs against Ostwald ripening and aggregation. These organic ligands exert a "barrier" effect on reagents and products limiting their access to (adsorption) and removal from (desorption) the catalytic surface, while on the other hand they provide chemical and colloidal stability to the catalyst.[4] Consequently, a compromise between activity and robustness (reusability) may require the use of ligands that cause a decrease in the performance of the catalysts but allow for longer durability.[22] Despite their crucial role in maintaining the stability of NCs, the impact of the ligand shell on both the final catalytic performance and reusability of NCs has been poorly studied, due in part to the difficulty in producing metal NCs with the same intrinsic parameters (composition, size and crystal structure) while presenting different surface coatings.[23, 24]

Herein, we present a comprehensive study on how the catalytic performance and reusability of colloidal dispersions of metal NCs are affected by systematic variations in size, composition, and surface coating using the reduction of organic dyes by borohydride ($NaBH_4$) ions as a model reaction (**Scheme 1**) (**see Fig. S1**). Due to its simplicity and the ease by which it can be monitored using UV-Vis spectroscopic techniques[25] this reaction has emerged as one of the most widely used system for assessing the catalytic (and photocatalytic) properties of nanostructured materials.[26-28] In particular, it takes place at room temperature only in the presence of the catalyst and has no known side reactions.[27] Therefore, high-precision real-time monitoring is possible by recording successive reductions in the characteristic absorbance maximum of the selected dye. Additionally, when carried out in excess of borohydride, the reaction can be understood in terms of the Langmuir-Hinshelwood (LH) model which allows the quantitative measurement of reaction rates and other kinetic parameters.[29] Furthermore, the use of monodisperse NCs allows estimating their total surface area (specific area) in solution with high precision, which can be directly used for determining the specific reaction constant per unit of surface area.

View Article Online
DOI: 10.1039/C7TA01328K

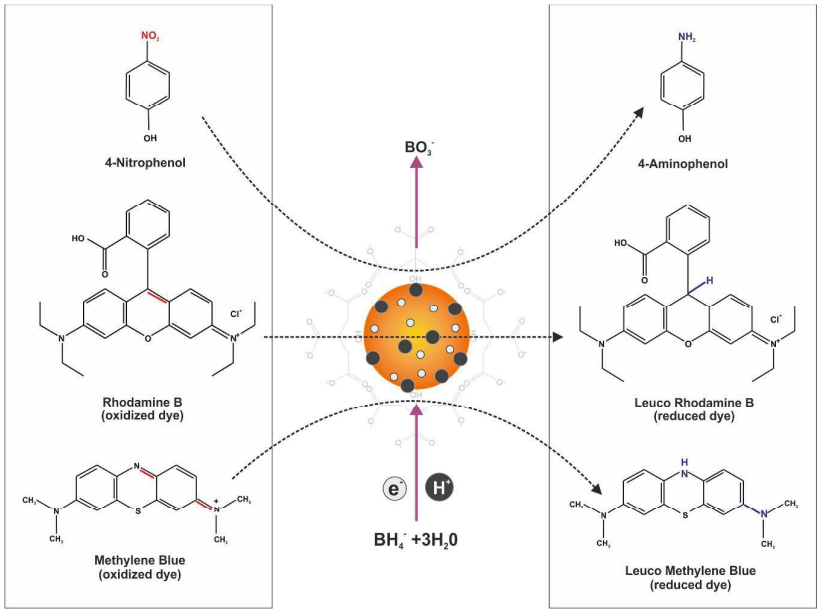

Scheme 1: Mechanism of the catalytic reduction and degradation of dyes used in this study. The catalytic reduction of dyes (4-Nitrophenol, Rhodamine B and Methylene Blue) by $NaBH_4$ is an electrochemical process in which the metal NCs have the main role of acting as electron relay systems, transferring the electrons from the donor (BH_4^-) to the acceptor (dye). BH_4^- ions are adsorbed on and react with the surface of metal NCs, thereby creating active metal hydrides at their surface. At the same time, the dye also adsorbs on the surface of metal NCs. Then electron transfer takes place between the dyes and BH_4^- through particle surface. After receiving the electrons, the dye molecules are reduced to 4-Aminophenol, Leuco Methylene Blue or Leuco Rhodamine B.

Taking advantage of the recent improvements in the colloidal synthesis of noble metal NCs, we have systematically studied these effects on highly monodisperse citrate-stabilized Au NCs of different sizes (from 3.6 to 110 nm).[30, 31] Due to the accurate morphological and chemical control of their surface (functionalization), these colloids are extremely interesting candidates for studying the impact of the surface nature of NCs in their final catalytic performance. We start first by analyzing the size-dependent catalytic activity of Au NCs followed by an analysis of how their catalytic performance is affected by modifications of Au NC surface chemistry. Finally, we extend this study to Ag and Pt NCs, aiming to understand how different materials present different catalytic performances. For completeness, we also evaluate this effect on different dyes in order to facilitate comparison and to evaluate the effects of charge and hydrophilicity of the dye. We believe that this study provides a better understanding of the catalytic performance of Au NCs upon controlled modifications of structural and morphological parameters, and working environment that can be used to facilitate the selection of the optimum NC size, coating molecules and evaluation systems for a particular study of interest.

View Article Online
DOI: 10.1039/C7TA01328K

RESULTS and DISCUSSION

Synthesis of Gold Nanocrystals

Colloidal aqueous solutions of Au NCs were produced following recently reported seeded-growth strategies.[30, 31] $HAuCl_4$ was used as an Au precursor and its reduction was achieved by the combined use of two competing reducing agents: sodium citrate (SC) and tannic acid (TA). Au NCs were coated with SC/TA molecules which provides a negative electrostatic stabilization once adsorbed onto the NC surface, allowing excellent dispersibility in aqueous media and easy post-synthetic functionalization. The growth of seed particles was kinetically controlled by adjusting the temperature of the reaction, the pH, the seed to Au precursor ratio, and the balance between both reducing agents. By controlling these synthetic parameters, successive generations of Au NCs with precisely controlled sizes (from 3.6 to 110 nm) and decreasing concentrations (from ~10^{14} NCs/mL to ~10^{10} NCs/mL, respectively) were obtained. Representative Transmission Electron Microscopy (TEM) images of selected Au NCs used in this study can be found in **Figure 1**, clearly showing their high monodispersity and narrow size distribution, with standard deviations below 10% (**see Fig. S2**).

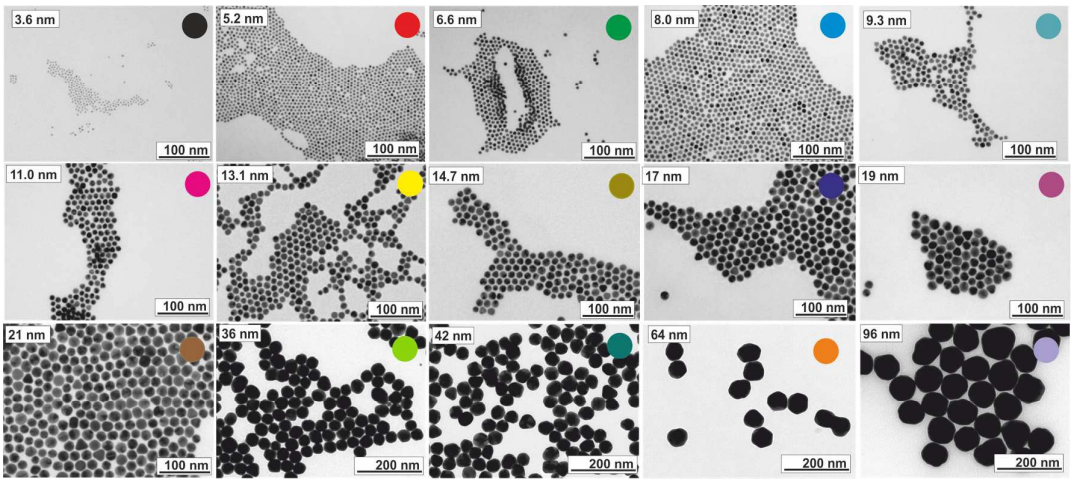

Figure 1: Representative transmission electron microscopy mages of citrate-stabilized Au NCs of selected particles ranging from 3.6 nm to 110 nm. Au NCs of 80.5 nm and 110 nm has been omitted from the figure. Color codes are visual aids corresponding to line plots in later figures.

For the deeper investigation of Au NCs and in order to discard facet-dependent effects, we analysed the morphology and crystal structure of selected NC sizes using high-resolution TEM (HRTEM) and high-angle annular dark field scanning TEM (HAADF-STEM)**.** Results shown in **Figure 2** suggest that Au NCs are faceted multiply twinned structures with decahedral or icosahedral geometry, all of them exposing the same {111} external facets. Interestingly, smaller Au NCs present a rounder decahedral shape while larger sizes have a morphology closer

View Article Online
DOI: 10.1039/C7TA01328K

to the ideal decahedron with sharper facets exposed. Finally, very large particles present an icosahedral structure with an increased number but identical {111} exposed facets. On the basis of the presented HRTEM observations, we propose a model to calculate and compare the variation of the ratio of surface active Au atoms with size (**see Fig. S3**). The 3D atomic modelling and simulation results can be found in the Supplementary Information **(Fig S7-S12).** Although the morphological differences observed, it is possible to conclude that the particular size-dependent catalytic performance obtained is not produced by differences in the crystal structure or the facets exposed by the Au NCs upon variations on their size.

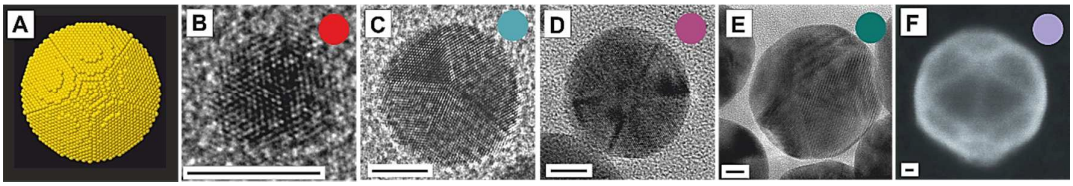

Figure 2. Representative HRTEM (B-E) and SEM (F) images showing the typical structure of Au NCs of 5.2 nm (B), 9.3 nm (C), 19 nm (D), 42 nm (E) and 96 nm (F) shown in Figure 1. Au NC from (B) to (E) show spheroidal decahedron morphology while (F) shows an icosahedral morphology. The image on the left (A) shows a 5.2 nm diameter 3D atomic simulation of a spheroidal decahedron.[32] Scale bars are 5 nm.

Size-dependent Catalytic Activity of Au Nanocrystals

The catalytic performance of Au NCs of different sizes was assessed for the reduction of 4-nitrophenol (4-NP) to 4-amoniphenol (4-AP) using sodium borohydride ($NaBH_4$) as the reducing agent.[33] The size range from 3.6 to 110 nm was covered by 17 different samples. Catalysis measurements were carried out using aqueous solutions of 4-NP and $NaBH_4$ concentrations of 0.16 mM and 6 mM, respectively. Reactants were pipetted into the cuvette in the sequence 4-NP, $NaBH_4$ and then the Au NCs to initiate the reaction. In our experiments, the pH of the solution was maintained at highly alkaline conditions (pH~10), which allows discarding the chemical decomposition of the $NaBH_4$ on the timescale of the catalyzed reaction.[27, 34] The total surface area of the NCs in solution was kept constant for the different sizes studied (0.5 cm^2/mL) by controlling the volume of Au NCs added to the reaction mixture. An accurate estimation of the surface area was obtained by considering the size distribution of the Au NCs used (see S2) and its concentration in solution. Every Au NC set was synthesized at least twice and the catalytic test reaction was repeated in triplicate for each set to ensure reproducibility.

The reduction process of 4-NP to 4-AP was monitored by measuring the temporal evolution of UV-Vis absorption spectra of the reaction mixture (**Fig. 3A-F**). The initially clear solution of 4-NP rapidly turned yellow immediately after the addition of $NaBH_4$, indicating the formation of

View Article Online
DOI: 10.1039/C7TA01328K

4-nitrophenolate ions (absorbance peak at ~400 nm) in the alkaline reducing medium caused by $NaBH_4$.[10, 26, 35, 36] Although the reduction of 4-NP by $NaBH_4$ is a thermodynamically feasible process, it is kinetically restricted and did not occurred even after 7 days, with the maximum absorption peak remaining unaltered in the absence of the catalyst.[37] The further addition of Au NCs catalyzed the transfer of electrons from BH_4^- to nitrophenolate ions, which was translated into a gradual decrease in the absorbance at 400 nm and the growing of a new absorbance band at 298 nm, associated with the formation of 4-AP. It is worth mentioning that in our working conditions, no optical interference with the absorption band of Au NCs was observed due to low spectral overlapping between both signals (**Fig. S6**) and the small volumes of Au NCs needed to catalyze the reaction (**Fig. 3A-F**). The presence of isosbestic points in the spectra of the reacting mixtures indicates that no side reactions occur.[38] Importantly, the concentration of BH_4^- ion greatly exceeded (~ 40-times higher) that of 4-NP and essentially remained constant during the process.[27] Therefore, the reaction followed pseudo-first order kinetics[39] with respect to the concentration of 4-NP. Despite still being a matter of debate,[33] this assumption has been made in previous studies.[19, 33, 40] Degradation rates were described in terms of the apparent reaction rate constant, k_{app}, determined for each sample from the negative slope of the linear on the $\ln(A/A_0)$ vs. time plot, where A/A_0 is the dye absorbance maximum normalized to its value at the initial time of reaction.[25]

Figure 3G shows the temporal evolution of the absorbance at 400 nm (4-nitrophenolate peak position) for all sizes studied. As can be seen, for very small sizes, the reduction of 4-NP is very fast, as evidenced by the fact that the absorption profile drops rapidly to zero. As particle size increases from 5.2 to 8 nm, their catalytic activity slightly decreases. Surprisingly, Au catalysts with sizes between 8 nm and 11 nm are more active for the investigated reaction than the Au NCs with smaller diameters. For larger Au NCs (from 13 to 110 nm), an increase in size is accompanied by a decrease in catalyst activity, on average three times lower than the smallest Au NCs studied. The specific reaction rates are given in **Figure 3H** and **Table 1**. k_{app} is highest for the smallest Au NCs studied (k= 0.444 min^{-1}), decreasing with increasing particle size except for the size range between 5.1 and 13.1 nm, where it first dropped reaching a minimum at 9.3 nm (k= 0.288 min^{-1}) and then increased again (k= 0.408 min^{-1}). This behavior results in an absolute maximum at 3.6 nm, the smallest size herein tested, and a relative maximum at 13.1 nm. In between, Au NCs present a lower performance.

Interestingly, this unexpected non-monotonic behavior was masked when obtained results were normalized to the elemental Au concentration in each sample (**Fig. 3J**) or to the total number of NCs in solution (**Fig. 3K**). Keeping constant the total number of Au atoms in solution, an overall decrease of the catalytic rate with size is observed, which can be explained considering that the total number of surface Au atoms exposed exponentially decreases as the size of the Au

View Article Online
DOI: 10.1039/C7TA01328K

catalyst increases, being much lower for larger Au NCs than for smaller ones.[41, 42] However, this decrease is faster than expected if the decrease of catalytic activity was only due to the reduction of the surface to volume ratio. Conversely, when the total number of particles (i.e., particle concentration) was kept constant, an increase of the k_{app} with size is found arising from the fact that a single, larger particle possesses higher surface area than a small one. Consequently, the exceptional behavior found for the small particle regime (3.6 to 13.1 nm) cannot be observed when normalizing the studies to the total Au concentration or particle number. This indicates that for the proper evaluation of intrinsic size effects at the nanoscale, the catalytic rates should be compared "per surface area" rather than comparing them "per particle" or "per weight", despite the fact that these parameters are the most commonly used to represent kinetic constants.[19, 20]

The size-dependent catalytic activity found in this study indicates that final catalytic performance is affected by the distinct surface reactivity of the Au NCs. Thus, Au atoms at the surface of small NCs are less coordinated than those of large particles and thus more reactive, nicely accounting for the general increase in their catalytic activity for decreasing sizes.[7, 41, 42] Unexpectedly, in our study this general trend partially reverts for sizes below 13.1 nm, indicating that small particles are less efficient in their catalytic performance than expected (**Fig. 2I)**. Analogous observations have been reported for similar and dissimilar systems[9, 19, 20, 43-45], attributing its origin to a combination of factors, including size-dependent charge transfer properties of the Au catalyst[46, 47] and size-dependent chemical interaction between the Au catalyst and the reactant.[19, 48] In this regard, it should be keep in mind that although the catalytic process is well-described by a LH kinetic model, the interaction of the dye with the metal NCs is a complex process greatly determined by the size of the NCs and the nature of the dye. Thus, a lower catalytic performance may be correlated with a less efficient electronic transfer to the catalytic Au site. As discussed by Fenger et al.[19] and further analyzed by others, a minimal Au surface area is required to adsorb planar dyes with its aromatic ring parallel to the surface (at least 6 gold atoms are needed for one 4-NP to adsorb[19]). This binding mode would prefer larger particles that have larger surface terraces. This ineffective binding may lead to a decrease in the catalytic performance that ultimately explain the observed size-dependent catalytic performance. Similarly, the less efficient performance can be also explained by a higher avidity of the small particles to interact with its surrounding environment, particularly with the molecules in their vicinity. Thus, it is widely known that less coordinated atoms tend to form stronger bonds with small molecules, being reported for instance how thiol-terminated ligands adsorb more strongly on small NCs than larger ones.[48] Therefore, as suggested by El-Sayed and co-workers[48], this stronger adsorption of reactant molecules on small NCs may block the reaction players from reaching the particle surface, resulting in a decrease in the catalytic

View Article Online
DOI: 10.1039/C7TA01328K

performance and consequently a lower reaction rate.[44] Finally, another important factor is the colloidal stability and integrity of the Au NCs as the coordination of surface atoms decreases.[7] This higher morphological instability of small particles is well-known, which is specifically critical at the liquid-solid interphase. Thus, small Au NCs more promptly undergo surface degradation processes such as corrosion,[49] and dissolution, as well as, aggregation and coalescence. All of these processes significantly alter the surface accessibility of the Au NCs, and therefore their catalytic performance. All of these hypothesis may account for the observed results in the small Au NC regime.

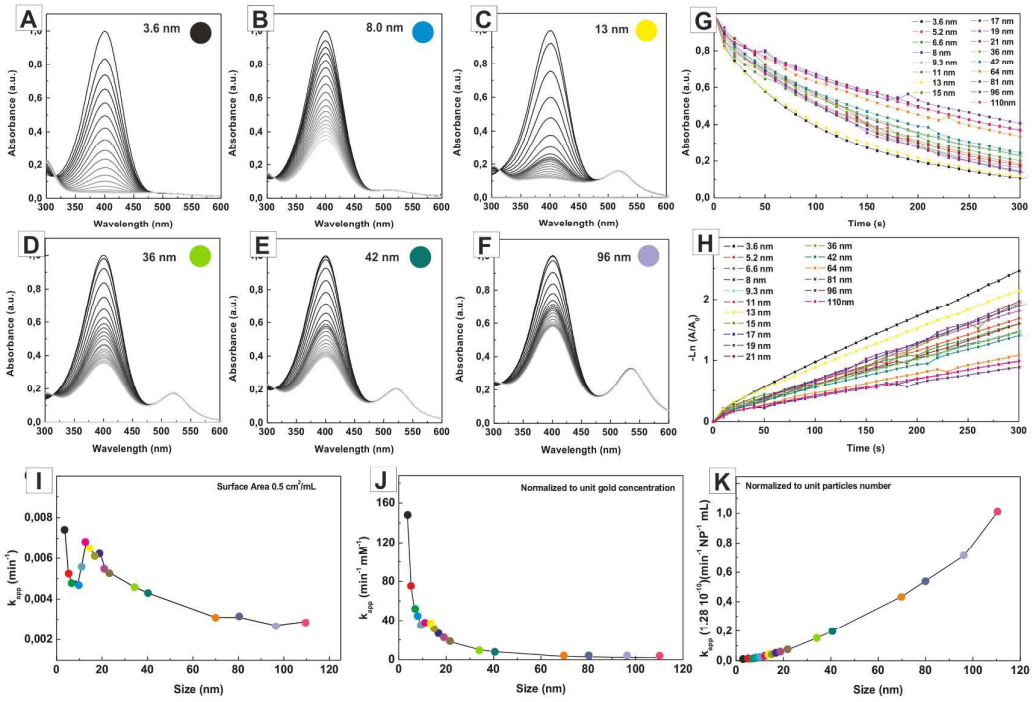

Figure 3: Time-dependent UV–visible spectra for the catalytic reduction of 4-NP by $NaBH_4$ in the presence of Au NCs of selected sizes (A) 3.6 nm, (B) 8.0 nm, (C) 13 nm, (D) 36 nm, (E) 42 nm, (F) 96 nm. Plot of time dependent absorbance 400 nm (G) and ln(At/A0) vs time for the eduction of 4-NP by $NaBH_4$ in the presence of Au NCs of different sizes. Comparative plots of k_{app} were obtained by keeping constant the total surface area of Au catalysts exposed (I), those normalized to the total Au atoms in solution (J) and particle number (K) for the different Au NCs solutions tested. In our working conditions, low spectral overlapping between the absorption band of 4-NP and Au NCs was observed due to the small volumes of Au NCs needed to catalyze the reaction.

Table 1: Size-dependent Catalytic Performance of Citrate-stabilized Gold Nanocrystals

	Pseudo first order rate constant					
	Constant Surface Area		**Normalized Au Atoms**		**Normalized Particle Number**	
Size (nm)	**k_{app} (min^{-1})**	**$k_{app*\ (size)/}$**	**k_{Au} (min^{-1}**	**k_{Au**}**	**k_{NC} (min^{-1}**	**$k_{NC***\ (size)/}$**

View Article Online
DOI: 10.1039/C7TA01328K

		$k_{app\ (3.6\ nm)}$	mM^{-1})	$_{(size)/}$ $k_{Au\ (3.6\ nm)}$	$NP^{-1}mL$)	$k_{NC\ (3.5\ nm)}$
3.6 ± 0.4	0.444	1	147.8	1	$3.57\ 10^{-13}$	1
5.2 ± 0.8	0.318	0.73	74.2	0.50	$5.27\ 10^{-13}$	1.47
6.6 ± 0.6	0.288	0.68	51.4	0.35	$7.58\ 10^{-13}$	2.12
8.0± 0.8	0.288	0.65	43.9	0.30	1.1110^{-12}	3.12
9.3 ± 1.0	0.282	0.64	35.6	0.24	$1.51\ 10^{-12}$	4.23
11.0± 1.0	0.336	0.76	36.6	0.25	$2.51\ 10^{-12}$	7.02
13.1 ± 1.1	0.408	0.92	37.8	0.26	$4.33\ 10^{-12}$	12.11
14.7 ± 1.2	0.39	0.88	31.8	0.22	$5.22\ 10^{-12}$	14.60
17 ± 1.4	0.366	0.82	25.8	0.18	$6.80\ 10^{-12}$	19.01
19.3 ± 1.5	0.378	0.85	23.5	0.16	$8.31\ 10^{-12}$	23.23
21.4 ± 1.5	0.324	0.73	18.0	0.12	$9.27\ 10^{-12}$	25.91
36 ± 3.1	0.276	0.62	9.9	0.07	$1.95\ 10^{-11}$	54.56
42.0± 3.7	0.258	0.58	8.1	0.05	$2.50\ 10^{-11}$	70.07
64.0 ± 6.4	0.186	0.42	3.2	0.02	$5.60\ 10^{-11}$	156.56
80.5 ± 6.8	0.186	0.42	2.7	0.02	$7.01\ 10^{-11}$	196.06
96.3 ± 8.1	0.162	0.36	2.0	0.01	$9.18\ 10^{-11}$	256.42
110.4 ± 8.5	0.174	0.39	1.9	0.01	$1.28\ 10^{-10}$	359.66

***kapp pseudo first order rate constant at equal total surface area 0.5 cm^2/mL**
**** km pseudo first order rate constant normalized at total mass k_{Au}=kapp/[Au]**
*****kn pseudo first order rate constant normalized at total number of particles $k_{NC}=k_{app}$/[NC]**

Reusability of Catalytic Nanocrystals

Robustness and stability are important factors when assessing the overall performance of a catalyst. In our study, size-dependent reusability was investigated by evaluating the repeated use of the Au NCs. The experiments for the degradation of 4-NP were performed six consecutive times, each time using the same Au NCs and a fresh dye solution. Results for two selected sizes, 3.6 nm and 9.3 nm, are shown in **Figure 4**. As can be seen in **Figure 4C-D,** larger Au NCs show relatively good catalytic activity after 6 reaction cycles which turns into minor variations (<8%) of its reaction rate constant after different cycles. On the contrary, the performance of small Au NCs is compromised after repeated use. Thus, their reaction rate constant decreases 50%, from 0.152 min^{-1} to 0.73 min^{-1}. This decrease in the efficiency for small Au NCs probably results from their lower structural stability, which may be attributed to their higher curvature radii.

Obtained results evidence the complex role of the surface nature in the evaluation of the overall catalytic performance of Au NCs. Although low-coordinated surface atoms in small NCs exhibit much higher catalytic activity due to a greater density of unsaturated atomic steps[12], these very active surface atoms may also be responsible for the deactivation of the catalyst. Thus, the small NCs have higher surface energies and hence a strong tendency to minimize their total surface

View Article Online
DOI: 10.1039/C7TA01328K

energy, which may be translated into surface reconstruction, sintering and eventually aggregation.[9] Alternatively, as previously discussed, this lower performance can be also ascribed to the stronger adsorption of reactant molecules on small NCs.[44] In this sense, a detailed design and study of catalysts functionalization NC is of fundamental importance in the development of improved catalysts. As mentioned before, a compromise between activity and reusability may require the use of ligands that cause a decrease in initial reaction rate but allow longer durability passivating the surface and providing robust colloidal stability.

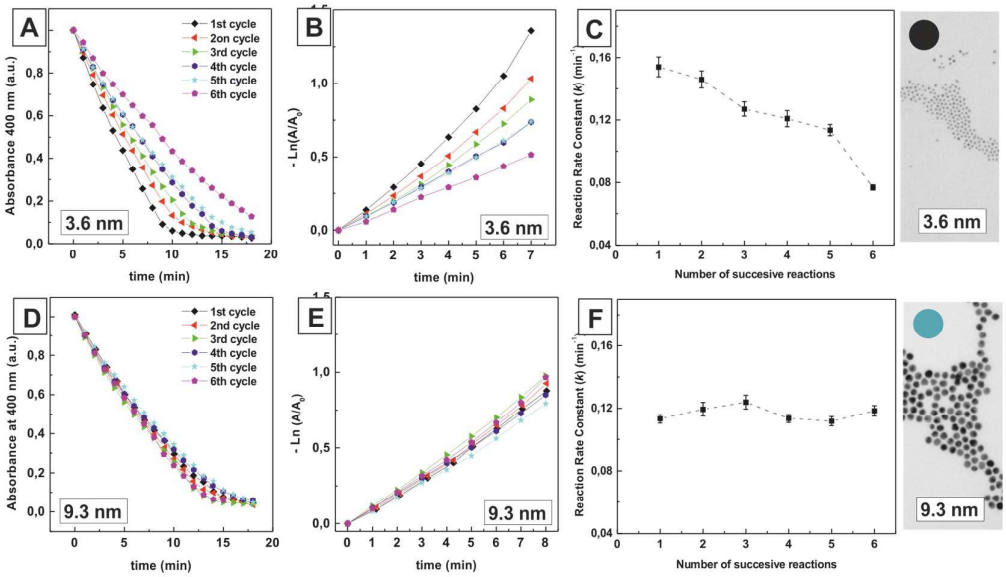

Figure 4: Evaluation of the reusability of Au NPs of different sizes. Plot of time-dependent absorbance 400 nm (A,D) and $\ln(A_t/A_0)$ vs. time (B,E) for the reduction of 4-NP by NaBH4 in the presence of Au NCs of different sizes: 3.6 nm (A,B) and 9.3 nm (D,E). Comparative plots of k_{app} obtained by keeping constant the total surface area of Au catalysts exposed vs. number of successive reaction cycles for Au NCs of 3.6 nm (C) and 9.3 nm (F).

Effect of Surface Coating

The effect of surface coating was studied by comparing the rates of the 4-NP reduction by $NaBH_4$ catalyzed by identical 3.6 nm Au NCs stabilized with different molecules: hexanoic acid (HA), aminohexanoic acid (AHA), polyethyleneglycol (PEG) of two different lengths (1000 and 3500 MW) and functional group (NH_2 and SH), polyvinylpyrrolidone (PVP, 40 KDa), mercaptoundecanoic acid (MUA) and bovine serum albumin (BSA). These ligands were chosen as model molecules due to their wide use and the special interest paid to them in material synthesis and functionalization.[50-53] Ligand exchange was performed by adding known amounts of molecules to Au NCs solutions under vigorous stirring. The mixture was allowed to react for 2 to 12 h (depending on molecule affinity) until no further peak evolution was detected by UV–vis spectroscopy.[54] Functionalized NCs were then centrifuged to remove excess of unreacted

View Article Online
DOI: 10.1039/C7TA01328K

molecules and finally re-dispersed in the same volume of milli-Q water. Characterization of Au NCs (**see Fig. S4**) shows that neither aggregation nor observable structural or morphological changes took place, indicating that the observed catalytic effects were due to modifications on NC surface chemistry.

The effect of surface coating in the catalytic performance of Au NCs is summarized in **Figure 5** and **Table 2**. As can be seen, a distinct decrease of the reduction rate of the dyes is observed after the functionalization of Au NCs with different molecules. Thus, as-synthesized SC/TA-stabilized Au NCs present the highest reaction rate constant, completely catalyzing 4-NP degradation in less than 20 min (**Fig. 5A**). In contrast, the reduction rate of dyes is decreased to a considerably extent for HA (**Fig. 5B**), AHA (**Fig. 5C**), and NH_2-PEG (1000)-coated Au NCs (**Fig. 5D**) having rate constants 3 times lower than those obtained for as-synthesized Au NCs (**Fig. 5I-K**). Finally, the functionalization of Au catalysts with MUA (**Fig. 5E**), PVP-40 (**Fig. 5F**), BSA (**Fig. 5G**) and SH-PEG(3500) (**Fig. 5H**) significantly blocked catalysis after some initial progress. As a result, the obtained reaction rates are up to 2 orders of magnitude lower than that obtained for as-synthesized Au NCs (**Fig. 5I-K**).

Obtained results indicate that the functionalization of Au NCs with different molecules compromise (to some extent) the performance of the catalysts. It is well-assumed that after functionalization Au NCs are surrounded by a dense coating layer which acts as a barrier for the reacting molecules consequently leading to a partial or complete loss of catalytic activity. Interestingly, the extent of this process is determined by the nature of the surfactant layer (degree of density, robustness and hydrophilicity) and can be explained, in a simplified manner, in terms of the physicochemical characteristics (length and anchor group) of the molecule tested. Thus, the catalytic performance depends on molecule length. Assuming a full surface coverage of the NC, short molecules provide a higher surface accessibility than larger ones, which is translated into higher catalytic performances. This is clearly seen in **Figure 4** where the reduction rate is distinctly slower in SH-PEG(3500) than in MUA. Both molecules present the same anchor group (SH) but different lengths (~7.9 nm vs ~2.4 nm). Similarly, the catalytic reduction rate is closely related to the nature of the chemical bonding between the molecule and the Au NCs. Thus, strongly bound molecules, such as SH-terminated ones, block more efficiently than weekly bound ones (NH2 or COOH) the reagents and reaction intermediates reaching the particle surface, thereby acting as a poison to the reaction and decreasing the rate of reaction. This is appreciated when comparing the catalytic performance of HA, AHA and MUA which differ in the anchor group, (i.e., the nature of the chemical bonding, HA (COOH-), AHA (NH_2-) and MUA (SH-)), while their length is similar (~1.3 nm for HA and AHA and ~2.4 nm for MUA) and much shorter than that of other molecules tested (NH_2-PEG(1000), ~4.3 nm) that present a higher catalytic performance. Other factors affecting the performance of

View Article Online
DOI: 10.1039/C7TA01328K

the catalysts are the charge and particular hydrophobicity/hydrophilicity of the molecule. As a result of the electrostatic interaction between the dye and the coating layer, the accessibility of the reacting molecules to the catalyst is more difficult for the dye when the surfactant carries the same charge due to electrostatic repulsion. Consequently, a larger decrease of the reaction rate is observed when the dye and the surfactant carry the same charge, while a smaller reduction of the reaction rate results is the dye and the surfactant are oppositely charged. Besides, the degree of molecule loading density and packaging along with the effectivity of the ligand exchange reaction determine the structure of the coating layer, which ultimately affects the performance of the catalyst.[55]

This surface-dependent reactivity of NCs has been widely reported for similar systems, including Au and Pd NCs coated with different organic molecules.[19, 23, 24, 56] An interesting point of these findings is the enhanced catalytic performance found after coating the Au NCs with hexadecyltrimethylammonium bromide (CTAB), widely used in the synthesis of Au NCs.[57-59] In our studies, this synergic effect was discarded when evaluating the catalytic performance of an aqueous solution of CTAB molecules (**see Fig. S5**), which showed that the molecules themselves are able to rapidly degrade 4-NP. These results emphasize the important role of the organic ligand in heterogeneous catalysis.[60] Similar controls were performed with all the ligands described in **Figure 5** with the result that catalysis did not occur even after 48 hours.

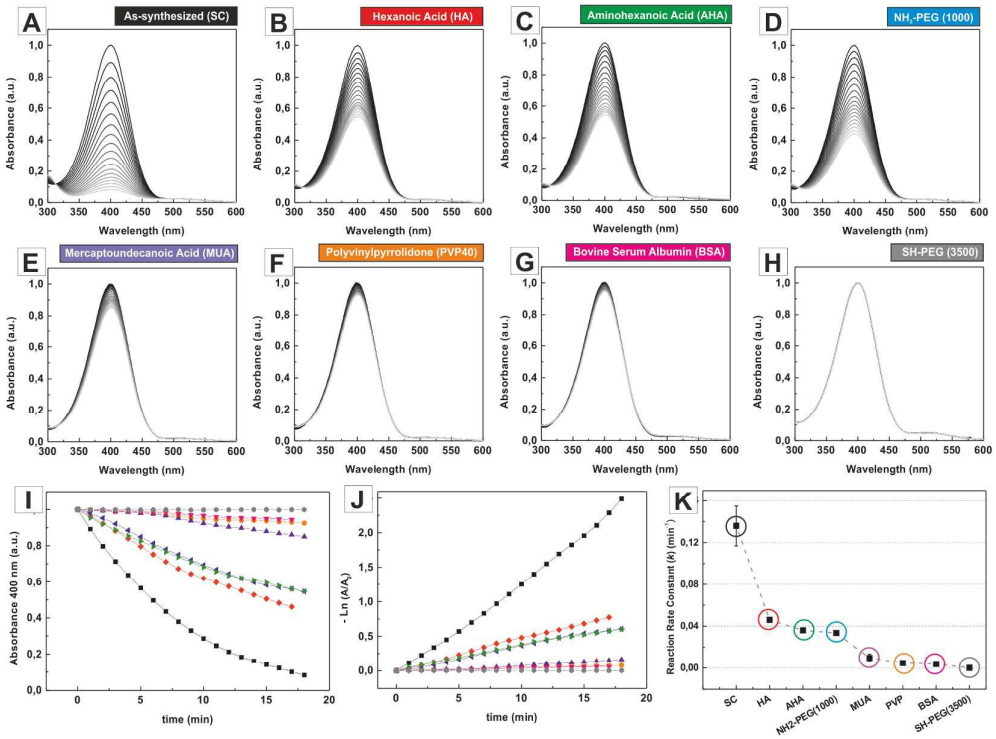

View Article Online
DOI: 10.1039/C7TA01328K

Figure 5. Influence of surface coating on the catalytic performance of Au NPs. The effect of surface coating was studied by comparing the rates of the 4-NP reduction by NaBH4 catalyzed by identical 3.6 nm Au NCs stabilized with different molecules: as-synthesized (A), hexanoic acid (B), aminohexanoic acid (C), NH_2-PEG (1000) (D), mercaptoundecanoic acid (E), polyvinylpyrrolidone (F), and bovine serum albumin (BSA) (H). Plot of time-dependent absorbance 400 nm (I) and $\ln(A_t/A_0)$ vs. time (J) for the reduction of 4-NP by $NaBH_4$ in the presence of Au NCs of 3.6 nm after their modifications of their surface coating. Comparative plots of kapp normalized to surface area vs. functionalization molecule (K).

Table 2: The Effect of the Coating Molecule on the Catalytic Performance of 3.6 nm Gold Nanocrystals**.**

	Pseudo first order rate constant	
Stabilizer	K_{app} (min^{-1})	$k_{s\ (ligand)*}$/ $k_{s\ (citrate)}$
SC	0.136	1
HA	0.046	0.34
AHA	0.036	0.26
NH2-PEG (1000)	0.034	0.25
MUA	0.010	0.07
PVP	0.005	0.03
BSA	0.004	0.03
SH-PEG (3500)	0.000	0.00

**k_{app} pseudo first order rate constant at equal total surface area

Effect of Dye andNanocrystal Composition

Beyond size and surface effects, the catalytic properties of Au NCs depend on the surrounding environment, particularly the model dye used as the testing system. In order to evaluate this influence, different organic dyes with well-defined spectral and electrochemical properties were used as probes. In addition to 4-NP, Methylene blue (MB) and Rhodamine B (RB) were chosen due to their wide use and their particular absorption profiles.[36] Each of them present a strong absorption signal in the UV-Vis regime. 4-NP has a maximum at 400 nm, RB at 554 nm and MB at 664 nm, which may interfere with the optical properties of the colloidal catalysts (**see Fig. S6**). The effects of the dye of choice and composition of the metal catalysts were studied by comparing the rates of 4-NP, RhB and MB reduction by $NaBH_4$ catalyzed by Au, Ag and Pt NCs **(Fig. 6A-I)**. Each catalyst solution consisted of ~20 nm PVP-capped NCs with a concentration of $4.2 \cdot 10^{12}$ NCs/mL, which allows the size and capping effect to be discarded. Moreover, to proper evaluate the stability of each dye in the presence of each catalyst, the dye concentration was kept constant.

View Article Online
DOI: 10.1039/C7TA01328K

Figure 6 shows the plot of the normalized decay of absorbance at each dye maximum as a function of time **(Fig. 6J-L)**, together with the negative natural logarithm from which k_{app} values were obtained **(Fig. 6M-O). These values are** summarized in **Table 3**. As can be seen, different concentrations of catalyst were needed to completely degrade each dye (50μL for 4-NP, 200 μL for RB and 5 μL for MB), suggesting that the reaction rate strongly depends on the dye used but not the overall response to variation of catalysts composition. MB appeared to degrade most promptly followed by 4-NP and then RB. As expected, the reaction rate depends on the composition of the catalysts used. In our explored conditions, the reactions catalyzed by Pt are systematically faster than those catalyzed by Au and Ag, independent of the dye. Thus, only 5 μL of Pt catalyst solution was needed to completely degrade the MB solution (**Fig.6I**), whereas Ag (**Fig.6F**) and Au (**Fig.6C**) showed a similar lower catalytic performance, with Au being slightly higher. Similar tendencies were found when using 4-NP. In this case, the concentration of Pt catalyst needed to completely degrade the 4-NP (**Fig.6G**) solution was 10-fold higher than with MB (**Fig.6I**). It is worth mentioning that, in our working conditions, no optical interferences were observed for Pt (**Fig.6G**) or Au (**Fig.6A**) due to the low volume of NCs needed to catalyze the reaction. Conversely, the high absorption signal of Ag NCs (**Fig.6D**), with a strong maximum surface plasmon resonance (SPR) band peaking at 400 nm, interferes with the dye signal. All this suggests that the evaluation of the catalytic activity of Ag with 4-NP is not suitable since high quantities of Ag catalysts were needed to complete the reaction, altering the absorbance signal and thereby providing unreliable results due to the difficulties in de-convoluting both signals. Despite Au NCs also contributing with a small absorbance peak at 520 nm, the significantly lower optical intensity does not mask the dye signal and can be practically discarded. Finally, among the three tested dyes, RB was the most difficult to reduce, evidenced by the fact that 200 μL of catalyst solution (40-fold higher than with MB) were needed to catalyze the reaction. As in the previous cases, Pt shows the highest activity (**Fig.6H**), followed by Au (**Fig.6B**), which is also significantly higher than Ag (**Fig.6E**).

View Article Online
DOI: 10.1039/C7TA01328K

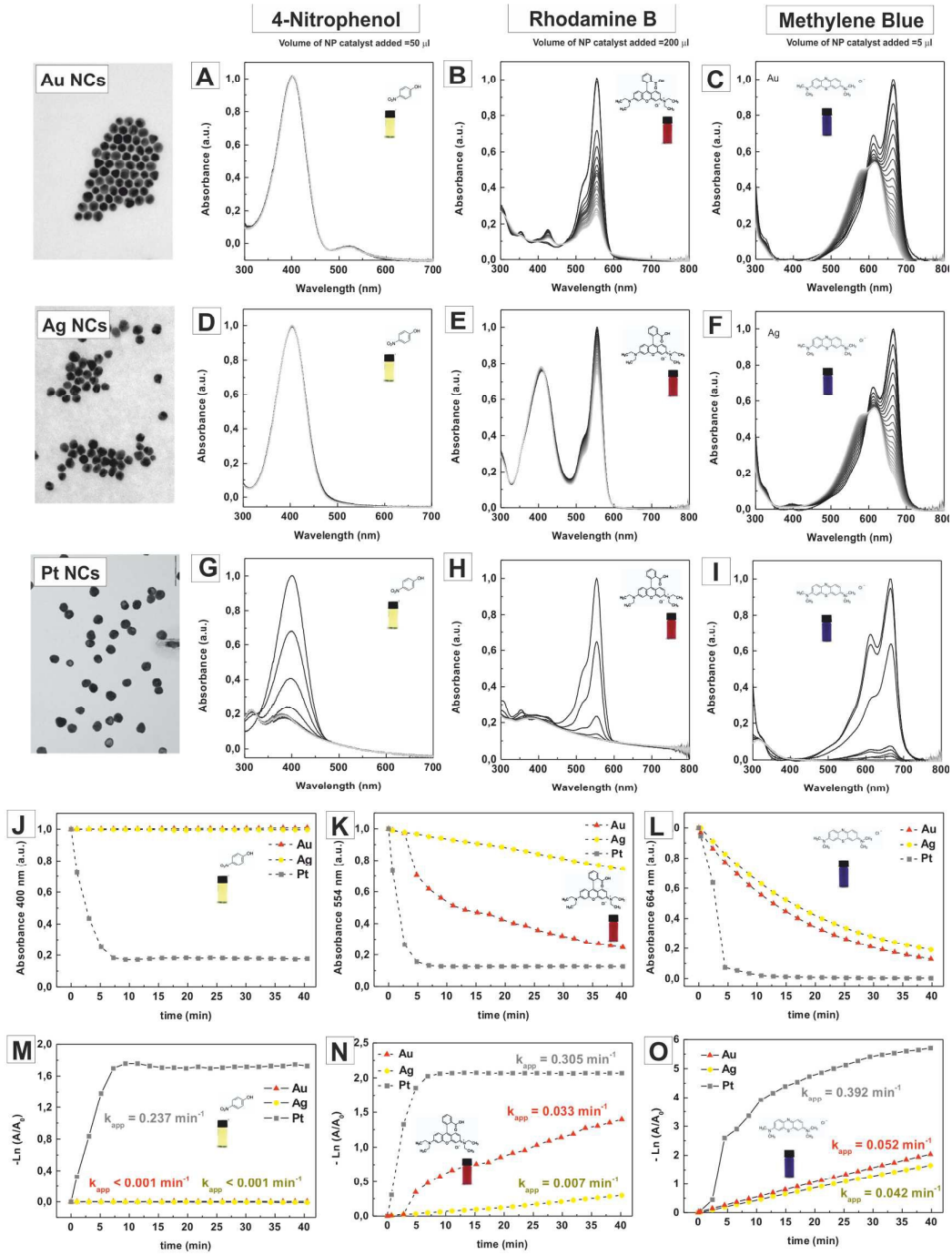

Figure 6. Influence of the dye on the catalytic performance of Au, Ag and Pt NCs. The effect of the model dye was studied by comparing the reduction rates of 3 model dyes (4-NP, RB and MB) by $NaBH_4$ catalyzed by identical 20 nm Au, Ag and Pt NCs stabilized with polyvinylpyrrolidone (A-I). Plot of time-dependent absorbance 400 nm (J-L) and ln(At/A0) vs. time (M-O) for the reduction of 4-NP, RB and MB by $NaBH_4$ in the presence of Au, Ag and Pt NCs of 20 nm after modifications of their surface coating with PVP.

View Article Online
DOI: 10.1039/C7TA01328K

Table 3. The Effect of the Dye on the Catalytic Performance of 20 nm Gold, Silver and Platinum Nanocrystals coated with PVP**.**

	Pseudo first order rate constant	
	k_s (min^{-1})	$k_{s\,(metal)}/\ k_{s\,(Au)}$
4-Nitrophenol		
Au	<0.001	1
Ag	<0.001	1
Pt	0.237	237
Rhodamine B		
Au	0.033	1
Ag	0.007	0.212
Pt	0.305	9.240
Methylene Blue		
Au	0.052	1
Ag	0.042	0.807
Pt	0.392	7.538

Conclusions

Au NCs with sizes ranging from 3.6 to 110 nm and with different functionalization were tested for their efficiency on the catalytic reduction of 3 different dyes (4-NP, RB and MB) with sodium borohydride. The catalytic performance of the Au NCs was found to be dependent on size, indicating that the performance is affected by the distinct surface reactivity of the Au NCs. As expected, the catalytic activity was also found to be strongly dependent on the nature of the coating molecule, obtaining increased catalytic activities for molecules that are weekly coordinated with the Au surface and compromised for molecules that are strongly absorbed. This lower catalytic activity for strongly bounded molecules was due to the blocking of the reaction players reaching the particle surface, mediated by the presence of strongly adsorbed molecules, thereby decreasing the rate of the reaction. Finally, results demonstrated that the catalytic performance of NCs depends on the surrounding environment, particularly the model dye used as the testing system and the NC chemical composition. The highest activity was found for MB, followed by 4-NP and RB. Besides, the reactions catalyzed by Pt are systematically faster than those catalyzed by Au and Ag, independent of the dye. We believe that this study provides an advance in basic understanding of NC catalytic properties and also a quantification of their response in performance and reusability to controlled modifications of structural, morphological and physicochemical parameters, and working environment. This knowledge can be used to select the optimum NC size, capping molecule and catalytic evaluation system for a particular study of interest, providing a framework through which the effects of potential system improvements can be assessed.

View Article Online
DOI: 10.1039/C7TA01328K

Acknowledgments

We acknowledge financial support from the Spanish Ministerio de Ciencia e Innovación (MICINN) (MAT2015-70725-R) and from the Catalan Agència de Gestió d'Ajuts Universitaris i de Recerca (AGAUR) (2014-SGR-612). Financial support from the FutureNanoNeeds (FP7-NMP-2013-LARGE-7) and HISENTS (685817) Projects financed by the European Community under the FP7 and H20202 Capacities Programme is gratefully acknowledged. N.G.B. acknowledges financial support by MINECO through the Ramon y Cajal program (RYC-2012-10991) and by the European Commission Seventh Framework Programme (FP7) through the Marie Curie Career Integration Grant (322153-MINE). ICN2 acknowledges support from the Severo Ochoa Program (MINECO, Grant SEV-2013-0295).

View Article Online
DOI: 10.1039/C7TA01328K

References

1. N. G. Bastús, E. Gonzalez, J. Esteve, J. Piella, J. Patarroyo, F. Merkoçi and V. Puntes, *Z. Phys. Chem.*, 2015, **229**, 65-83.

2. L. K. Bogart, G. Pourroy, C. J. Murphy, V. Puntes, T. Pellegrino, D. Rosenblum, D. Peer and R. Levy, *ACS Nano*, 2014, **8**, 3107-3122.

3. M. V. Kovalenko, L. Manna, A. Cabot, Z. Hens, D. V. Talapin, C. R. Kagan, V. I. Klimov, A. L. Rogach, P. Reiss, D. J. Milliron, P. Guyot-Sionnnest, G. Konstantatos, W. J. Parak, T. Hyeon, B. A. Korgel, C. B. Murray and W. Heiss, *ACS Nano*, 2015, **9**, 1012-1057.

4. Y. Wu, D. Wang and Y. Li, *Chem. Soc. Rev.*, 2014, **43**, 2112-2124.

5. Y. Xia, H. Yang and C. T. Campbell, *Acc. Chem. Res.*, 2013, **46**, 1671-1672.

6. H.-L. Jiang and Q. Xu, *J. Mater. Chem.*, 2011, **21**, 13705-13725.

7. N. G. Bastús, E. Casals, I. Ojea, M. Varon and V. Puntes, in *The Delivery of Nanoparticles*, ed. A. A. Hashim, InTech, 2012, DOI: DOI: 10.5772/35238.

8. M. Haruta, *Catal. Today*, 1997, **36**, 153-166.

9. R. Reske, H. Mistry, F. Behafarid, B. Roldan Cuenya and P. Strasser, *J. Am. Chem. Soc.*, 2014, **136**, 6978-6986.

10. E. Gonzalez, F. Merkoci, R. Arenal, J. Arbiol, J. Esteve, N. G. Bastus and V. Puntes, *J. Mater. Chem. A*, 2016, **4**, 200-208.

11. K. M. Bratlie, H. Lee, K. Komvopoulos, P. Yang and G. A. Somorjai, *Nano Lett.*, 2007, **7**, 3097-3101.

12. Y. Xiong, B. J. Wiley and Y. Xia, *Angewandte Chemie International Edition*, 2007, **46**, 7157-7159.

13. M. A. Mahmoud, R. Narayanan and M. A. El-Sayed, *Acc. Chem. Res.*, 2013, **46**, 1795-1805.

14. M. Valden, X. Lai and D. W. Goodman, *Science*, 1998, **281**, 1647-1650.

15. H. Tsunoyama, H. Sakurai, Y. Negishi and T. Tsukuda, *J. Am. Chem. Soc.*, 2005, **127**, 9374-9375.

16. H. Song, R. M. Rioux, J. D. Hoefelmeyer, R. Komor, K. Niesz, M. Grass, P. Yang and G. A. Somorjai, *J. Am. Chem. Soc.*, 2006, **128**, 3027-3037.

17. J. Jia, K. Haraki, J. N. Kondo, K. Domen and K. Tamaru, *J. Phys. Chem. B*, 2000, **104**, 11153-11156.

18. P. L. Freund and M. Spiro, *J. Phys. Chem.*, 1985, **89**, 1074-1077.

19. R. Fenger, E. Fertitta, H. Kirmse, A. F. Thunemann and K. Rademann, *Phys. Chem. Chem. Phys.*, 2012, **14**, 9343-9349.

20. T. K. Sau, A. Pal and T. Pal, *J. Phys. Chem. B*, 2001, **105**, 9266-9272.

View Article Online
DOI: 10.1039/C7TA01328K

21. C. Deraedt, L. Salmon, S. Gatard, R. Ciganda, R. Hernandez, J. Ruiz and D. Astruc, *Chemical Communications*, 2014, **50**, 14194-14196.

22. D. Astruc, F. Lu and J. R. Aranzaes, *Angewandte Chemie International Edition*, 2005, **44**, 7852-7872.

23. Y. Li and M. A. El-Sayed, *J. Phys. Chem. B*, 2001, **105**, 8938-8943.

24. R. Ciganda, N. Li, C. Deraedt, S. Gatard, P. Zhao, L. Salmon, R. Hernandez, J. Ruiz and D. Astruc, *Chemical Communications*, 2014, DOI: 10.1039/c4cc04454a.

25. P. Herves, M. Perez-Lorenzo, L. M. Liz-Marzan, J. Dzubiella, Y. Lu and M. Ballauff, *Chem. Soc. Rev.*, 2012, **41**, 5577-5587.

26. T. Aditya, A. Pal and T. Pal, *Chemical Communications*, 2015, **51**, 9410-9431.

27. S. Carregal-Romero, J. Pérez-Juste, P. Hervés, L. M. Liz-Marzán and P. Mulvaney, *Langmuir*, 2009, **26**, 1271-1277.

28. I. K. Konstantinou and T. A. Albanis, *Applied Catalysis B: Environmental*, 2004, **49**, 1-14.

29. S. Wunder, F. Polzer, Y. Lu, Y. Mei and M. Ballauff, *J. Phys. Chem. C*, 2010, **114**, 8814-8820.

30. N. G. Bastus, J. Comenge and V. Puntes, *Langmuir*, 2011, **27**, 11098-11105.

31. J. Piella, N. G. Bastús and V. Puntes, *Chem. Mater.*, 2016, **28**, 1066-1075.

32. http://gaen.cat/research/295

33. M. Li and G. Chen, *Nanoscale*, 2013, **5**, 11919-11927.

34. M. Chatenet, F. Micoud, I. Roche and E. Chainet, *Electrochim. Acta*, 2006, **51**, 5459-5467.

35. N. Pradhan, A. Pal and T. Pal, *Langmuir*, 2001, **17**, 1800-1802.

36. N. G. Bastús, F. Merkoçi, J. Piella and V. Puntes, *Chem. Mater.*, 2014, **26**, 2836-2846.

37. A. Gangula, R. Podila, R. M, L. Karanam, C. Janardhana and A. M. Rao, *Langmuir*, 2011, **27**, 15268-15274.

38. Y. Mei, Y. Lu, F. Polzer, M. Ballauff and M. Drechsler, *Chem. Mater.*, 2007, **19**, 1062-1069.

39. S. Wunder, Y. Lu, M. Albrecht and M. Ballauff, *ACS Catalysis*, 2011, **1**, 908-916.

40. M. Dasog, W. Hou and R. W. J. Scott, *Chemical Communications*, 2011, **47**, 8569-8571.

41. S. Panigrahi, S. Basu, S. Praharaj, S. Pande, S. Jana, A. Pal, S. K. Ghosh and T. Pal, *J. Phys. Chem. C*, 2007, **111**, 4596-4605.

42. Y. Mei, G. Sharma, Y. Lu, M. Ballauff, M. Drechsler, T. Irrgang and R. Kempe, *Langmuir*, 2005, **21**, 12229-12234.

View Article Online
DOI: 10.1039/C7TA01328K

43. C. Lin, K. Tao, D. Hua, Z. Ma and S. Zhou, *Molecules*, 2013, **18**, 12609.

44. Y. Li, E. Boone and M. A. El-Sayed, *Langmuir*, 2002, **18**, 4921-4925.

45. L. Yan, Y. Liu, K. Zha, H. Li, L. Shi and D. Zhang, *ACS Applied Materials & Interfaces*, 2017, **9**, 2581-2593.

46. M. M. Kappes, *Chem. Rev.*, 1988, **88**, 369-389.

47. K. Rademann, B. Kaiser, U. Even and F. Hensel, *Phys. Rev. Lett.*, 1987, **59**, 2319-2321.

48. B. L. Smith and J. E. Hutchison, *J. Phys. Chem. C*, 2013, **117**, 25127-25137.

49. M. Varon, I. Ojea-Jimenez, J. Arbiol, L. Balcells, B. Martinez and V. F. Puntes, *Nanoscale*, 2013, **5**, 2429-2436.

50. A. Yazdi, F. Mercoçi, N. G. Bastús, I. Imaz, V. Puntes and D. Maspoch, *Catalysis Science & Technology*, 2016.

51. E. Casals, T. Pfaller, A. Duschl, G. J. Oostingh and V. Puntes, *ACS Nano*, 2010, **4**, 3623-3632.

52. T. Yu, J. Zeng, B. Lim and Y. Xia, *Adv. Mater.*, 2011, **22**, 5188-5192.

53. J. Zeng, Q. Zhang, J. Chen and Y. Xia, *Nano Lett.*, 2010, **10**, 30-35.

54. N. G. Bastus, J. Piella and V. Puntes, *Langmuir*, 2016, **32**, 290-300.

55. S. M. Ansar and C. L. Kitchens, *ACS Catalysis*, 2016, **6**, 5553-5560.

56. A. Quintanilla, V. C. L. Butselaar-Orthlieb, C. Kwakernaak, W. G. Sloof, M. T. Kreutzer and F. Kapteijn, *Journal of Catalysis*, 2010, **271**, 104-114.

57. N. R. Jana, L. Gearheart and C. J. Murphy, *Langmuir*, 2001, **17**, 6782-6786.

58. N. R. Jana, L. Gearheart and C. J. Murphy, *J. Phys. Chem. B*, 2001, **105**, 4065-4067.

59. J. Pérez-Juste, I. Pastoriza-Santos, L. M. Liz-Marzán and P. Mulvaney, *Coordination Chemistry Reviews*, 2005, **249**, 1870-1901.

60. Z. Niu and Y. Li, *Chem. Mater.*, 2013, **26**, 72-83.

61. J. Arbiol, A. Cirera, F. Peiró, A. Cornet, J. R. Morante, J. J. Delgado and J. J. Calvino, *Applied Physics Letters*, 2002, **80**, 329-331.

62. S. Bernal, J. Calvino, M. Cauqui, J. P. Omil, J. Pintado and J. Rodrıguez-Izquierdo, *Applied Catalysis B: Environmental*, 1998, **16**, 127-138.

View Article Online
DOI: 10.1039/C7TA01328K

EXPERIMENTAL METHODS:

Chemicals. Sodium citrate tribasic dihydrate (≥99%), gold (III) chloride trihydrate $HAuCl_4 \cdot 3H_2O$ (99.9% purity), tannic acid (ACS reagent), 4-nitrophenol solution (10 mM), Rhodamine B (≥95%), Methylene blue, sodium borohydride (99.99%), hexanoic acid (99%), 6-Aminohexanoic acid (≥98.5%), 11-mercaptoundecanoic acid (98%), polyvinylpyrrolidone (MW 40000), poly(ethylene glycol) 2-aminoethyl ether acetic acid ($M_W \approx 1000$ g/mol, $n = 22$) (NH_2-PEG1000-COOH), poly(ethylene glycol) 2-mercaptoethyl ether acetic acid ($M_W \approx 3500$ g/mol, $n = 77$) (SH-PEG3500-COOH), 11-mercaptoundecanoic acid and bovine serum albumin (BSA) were purchased from Sigma-Aldrich. All reagents were used as received without further purification and all glass material was sterilized and dehydrogenated in an oven prior to use. Mili-Q water was used in the preparation of all solutions.

Nanoparticle Synthesis. Aqueous solutions of citrate-stabilized Au NCs with different sizes (3.6-110 nm) were synthetized according to previously developed seeded-growth methods in our group. Detailed synthetic procedure and full characterization of the resultant solutions can be found in the respective articles.[30, 31] Briefly, Au NCs with increasing sizes were obtained from an initial Au NC solution after different sequential steps of growing; consisting in sample dilution plus further addition of gold precursor. Consequently, the number of particles in the solution decrease as it size increase. In detail, the concentration of small 3.6 nm particles was 10^{14}, which decreased down to 10^{10} NCs/mL for the largest 110 nm particles. All the particles were used within 20 days from their synthesis. A similar seeded-growth strategy has been followed to produce citrate-stabilized Ag NCs.[36] Resultant NCs were purified by centrifugation (10 000g to 18 000g, depending on its size) acid and further redispersed in Milli-Q-water or sodium citrate 2.2 mM before sample characterization and ligand exchange experiments. Pt NC surfaces were produced via galvanic replacement reaction (GRR) using PVP-coated 20 nm Ag NPs as a sacrificial templates.[10]

Ligand Exchange of Nanoparticles. For ligand exchange experiments, aqueous solutions of (i) hexanoic acid (99%), (ii) 6-Aminohexanoic acid (≥98.5%), (iii) 11-mercaptoundecanoic acid (98%), (iv) polyvinylpyrrolidone (MW 40000), (v) poly(ethylene glycol) 2-aminoethyl ether acetic acid ($M_W \approx 1000$ g/mol, $n = 22$) (NH_2-PEG1000-COOH), (vi) poly(ethylene glycol) 2-mercaptoethyl ether acetic acid ($M_W \approx 3500$ g/mol, $n = 77$) (SH-PEG3500-COOH), and (vii) bovine serum albumin (BSA) were prepared and added to as-synthesized citrate-stabilized Au NCs solutions under vigorous stirring (final concentration 0.5 mM). The mixture was allowed to react for 2 h (SH-PEG3500-COOH, MUA) or 12 h (HA, AHA, PVP40, NH_2-PEG1000-COOH, BSA), and resultant NCs were then centrifuged to remove excess of unreacted molecules and finally redispersed in the same volume of milli-Q water.[54]

Characterization: NCs were characterized by transmission electron microscopy (TEM, JEOL 1010) and UV-vis spectroscopy (Shimazu, 2010). All the 3D atomic models presented in this work have been created by using the Rhodius software.[61, 62] The morphological and structural characterizations of the nanocrystals were carried out by high-resolution TEM (HRTEM). HRTEM images were obtained using a FEI Tecnai F20 field-emission gun microscope with a 0.19 nm point-to-point resolution operated at 200 keV.

Catalytic Reaction: The standard catalytic test reaction was carried out in 4.5 mL PS-disposable cuvettes. Aqueous solutions of 4-nitrophenol (4-NP), methylene blue (MB) or rhodamine B (RB) (1 mM) were prepared as received. $NaBH_4$ solution (0.1 M, pH = 10.6) was

View Article Online
DOI: 10.1039/C7TA01328K

freshly prepared before each set of kinetic trials. Experimentally, 2mL of milliQ water, 30-75 μL of dye solution and 100μL of $NaBH_4$ solution were sequentially added into a PS-disposable cuvette. Then, an aqueous solution containing Au NCs (normalized in terms of surface area) was injected into the cuvette to start the reaction. The absorbance of each organic dye was monitored by UV-Vis spectroscopy as a function of time (20 runs, each 60 seconds) in the 300 nm to 800 nm range at room temperature.

Calculation of Kinetic Rate Constants: Apparent kinetic constant rates were obtained according to the first-order rate law in which the intensity of the signal was firstly normalized to the maximum of absorbance of each dye (400 nm, 554 nm and 664 for 4-NP, RB and MB, respectively) and then the negative natural logarithm was plotted as a function of time, where the steepest part of the curve was linearly fitted, the slope of which was considered the apparent rate constant k_{app}. The rate constant is considered apparent because previous work by other groups has shown that the observed rate constant depends on the concentration of $NaBH_4$ as well as the starting concentration of 4-nitrophenol.[39] Each measurement was performed per triplicate to evaluate its reproducibility.